

HSViT: Horizontally Scalable Vision Transformer

Chenhao Xu

chenhao.xu@deakin.edu.au

School of Information Technology, Deakin University
Geelong, VIC, Australia

Chee Peng Lim

chee.lim@deakin.edu.au

Institute for Intelligent Systems Research and Innovation,
Deakin University
Geelong, VIC, Australia

Chang-Tsun Li*

changtsun.li@deakin.edu.au

School of Information Technology, Deakin University
Geelong, VIC, Australia

Douglas Creighton

douglas.creighton@deakin.edu.au

Institute for Intelligent Systems Research and Innovation,
Deakin University
Geelong, VIC, Australia

ABSTRACT

While the Vision Transformer (ViT) architecture gains prominence in computer vision and attracts significant attention from multimedia communities, its deficiency in prior knowledge (inductive bias) regarding shift, scale, and rotational invariance necessitates pre-training on large-scale datasets. Furthermore, the growing layers and parameters in both ViT and convolutional neural networks (CNNs) impede their applicability to mobile multimedia services, primarily owing to the constrained computational resources on edge devices. To mitigate the aforementioned challenges, this paper introduces a novel horizontally scalable vision transformer (HSViT). Specifically, a novel image-level feature embedding allows ViT to better leverage the inductive bias inherent in the convolutional layers. Based on this, an innovative horizontally scalable architecture is designed, which reduces the number of layers and parameters of the models while facilitating collaborative training and inference of ViT models across multiple nodes. The experimental results depict that, without pre-training on large-scale datasets, HSViT achieves up to 10% higher top-1 accuracy than state-of-the-art schemes, ascertaining its superior preservation of inductive bias. The code is available at <https://github.com/xuchenhao001/HSViT>.

CCS CONCEPTS

• **Computing methodologies** → **Computer vision**.

KEYWORDS

Vision Transformer, Image-Level Feature Embedding, Horizontal Scaling, Convolutional Neural Network, Computer Vision

ACM Reference Format:

Chenhao Xu, Chang-Tsun Li, Chee Peng Lim, and Douglas Creighton. 2024. HSViT: Horizontally Scalable Vision Transformer. In *Proceedings of ACM Conference'17, July 2017, Washington, DC, USA*

*Chang-Tsun Li is the corresponding author.

Permission to make digital or hard copies of all or part of this work for personal or classroom use is granted without fee provided that copies are not made or distributed for profit or commercial advantage and that copies bear this notice and the full citation on the first page. Copyrights for components of this work owned by others than the author(s) must be honored. Abstracting with credit is permitted. To copy otherwise, or republish, to post on servers or to redistribute to lists, requires prior specific permission and/or a fee. Request permissions from [permissions@acm.org](https://permissions.acm.org).
Conference'17, July 2017, Washington, DC, USA

© 2024 Copyright held by the owner/author(s). Publication rights licensed to ACM.
ACM ISBN 978-x-xxxx-xxxx-x/YY/MM... \$15.00
<https://doi.org/XXXXXXXX.XXXXXXX>

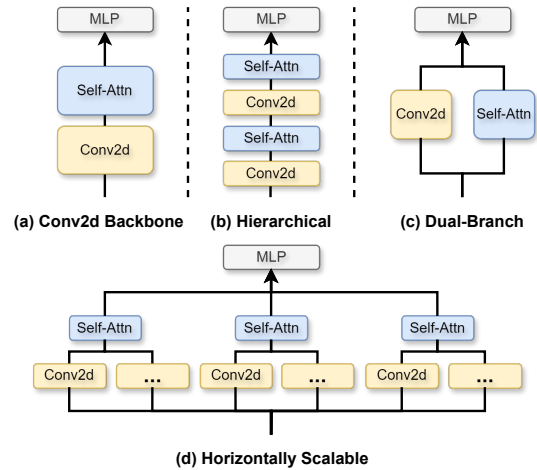


Figure 1: Comparison of various hybrid ViT architectures. HSViT exhibits superior horizontal scalability and the flexibility to be applied on multiple resource-constrained devices.

Conference (Conference'17). ACM, New York, NY, USA, 9 pages. <https://doi.org/XXXXXXXX.XXXXXXX>

1 INTRODUCTION

The ubiquity of smartphones, tablets, and wearable devices has led to an increased demand for intelligent mobile multimedia services [11, 19]. Augmented reality (AR) applications, for instance, require sophisticated analysis of real-world visual environments (content understanding) to enhance user experience [4]. With deep learning models demonstrating superior performance compared to traditional algorithms across various Computer Vision (CV) tasks, researchers and practitioners are increasingly leveraging these models to deliver smarter multimedia services [19].

The remarkable success of the self-attention mechanism in Natural Language Processing (NLP) [27] has sparked a surge of research interest in Transformer-based CV models, such as the Vision Transformer (ViT) [8]. These ViT models have yielded impressive performance across various CV tasks, including image classification, object detection, and segmentation [33], owing to their ability to capture long-range dependencies among visual features across

the entire image [22]. However, ViTs typically require tedious pre-training on large-scale datasets to achieve their superior performance [8].

The need for pre-training ViTs stems from their lack of inductive biases similar to those present in convolutional neural networks (CNNs) [6, 22]. Specifically, CNNs inherently incorporate several inductive biases that make them well-suited for CV tasks, such as translation invariance, spatial locality, and hierarchical feature learning [29]. By contrast, ViTs divide images into a sequence of fixed-sized non-overlapping patches and introduce positional encodings to these patches [8]. These patch-level feature embeddings pose challenges for the self-attention layers in capturing spatial invariances [22]. Consequently, to harness the ability of self-attention with respect to capturing long-range dependencies in image features while preserving the inductive biases of CNNs, integrating self-attention mechanisms with convolutional layers presents a promising solution.

As shown in Fig. 1, there are primarily three types of hybrid ViT: convolutional backbone, hierarchical, and dual-branch architectures. The convolutional backbone and dual-branch architecture typically add a full-size CNN to the ViT model, increasing the number of model parameters and computational burden [2, 20]. The hierarchical design usually incorporates multiple self-attention layers into classic CNNs to build a hierarchical feature extraction structure [13, 18, 25, 29]. While the self-attention layers help CNNs learn long-range feature dependencies in images across different levels, they disrupt the inductive bias of CNNs and necessitate pre-training.

To address the aforementioned challenges, this paper presents a novel Horizontally Scalable Vision Transformer (HSViT). First, a new image-level feature embedding for ViT is designed to better utilize the inductive biases from convolutional layers. In particular, multiple convolutional kernels operate concurrently on the same image, with each kernel extracting a corresponding feature within the context of the entire image. The features are hierarchically downsampled using max pooling to a fixed size, preserving the inductive biases to the greatest extent. Then, each feature map is flattened as an embedding of the Transformer, allowing the self-attention mechanism to construct long-range dependencies among distinct image-level features.

Second, upon the image-level feature embeddings, a novel horizontally scalable self-attention architecture is designed, leveraging the computing resources across nodes to handle more features. The comparison between the horizontally scalable architecture with other hybrid ViT architectures is shown in Fig. 1. Specifically, the flattened feature maps are divided into several attention groups, with self-attention computed within each group. Then, the predictions from these attention groups are aggregated to yield a final prediction. The horizontally scalable design effectively reduces the number of layers and parameters of the model, as shown in Fig. 2. A series of experiments conducted on five small image classification benchmark datasets demonstrate that, without pre-training on large-scale datasets, HSViT achieves up to 10% higher top-1 accuracy than the state-of-the-art CNN and ViT schemes.

The main contributions of this paper are summarized as follows:

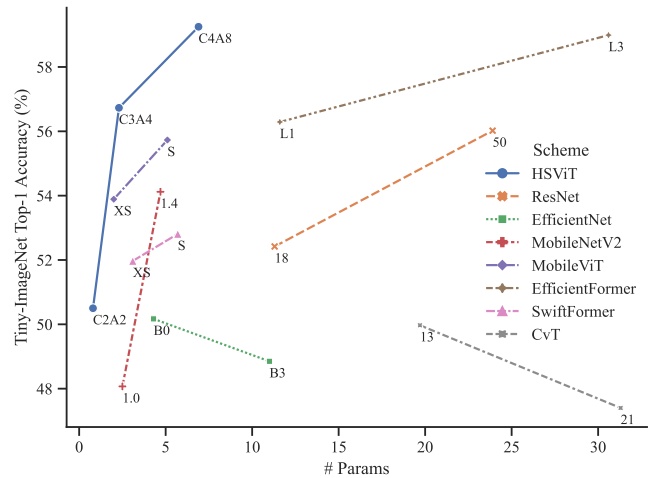


Figure 2: Number of parameters vs. Tiny-ImageNet top-1 accuracy (%). HSViT achieves higher top-1 accuracy on Tiny-ImageNet with fewer model parameters, due to image-level feature embeddings and horizontally scalable self-attention architecture.

- A novel image-level feature embedding for ViT is proposed, which largely preserves the inductive biases present in convolutional layers and mitigates pre-training requirements.
- A horizontally scalable self-attention architecture is designed, which reduces the number of layers and parameters of the model while better utilizing computing resources across multiple nodes.
- A series of experiments validate that HSViT better preserves inductive biases and outperforms state-of-the-art models in terms of top-1 accuracy while requiring fewer layers and parameters.

2 RELATED WORK

Vision Transformer: Transformer and its self-attention mechanism [27] are introduced to CV after their success in NLP, and achieve better performance than their CNN counterparts in a variety of tasks with the help of pre-training on large-scale datasets [2, 8]. Nevertheless, as the images are converted into patch-level embedding sequences, the complexity of self-attention in ViTs is quadratic to the product of image height and width, leading to a huge number of model parameters and significant computing overhead. Numerous approaches have been proposed to address this challenge, such as window-based attention [14, 15], sparse attention [5, 31], low-rank approximations [3], model pruning and quantization [16, 35], etc. All these schemes adhere to the patch-level feature embedding design in ViT. By contrast, this paper proposes a novel image-level feature embedding for ViT, leading to a large reduction in the number of layers and parameters and superior horizontal scalability.

Hybrid Vision Transformer: Convolutional layers are well recognized to assist ViTs in capturing local spatial patterns and learning hierarchical representations of spatial features in images. As a result, many hybrid vision transformer architectures that integrate convolutional layers with self-attention layers have been

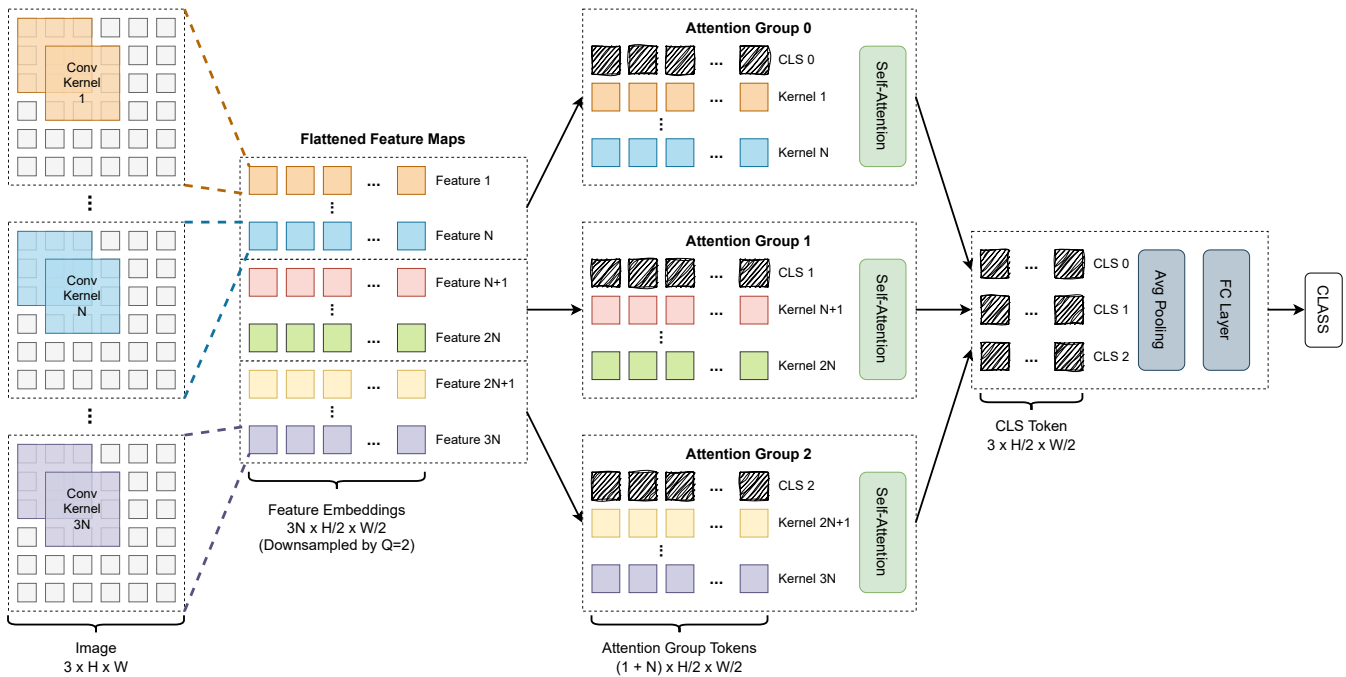


Figure 3: Feature processing pipeline of HsviT.

proposed, including convolutional backbone [2, 7, 8, 13], hierarchical [9, 18, 25, 29], and dual-branch architectures [20, 36], as shown in Fig. 1. In particular, convolutional backbone architectures, like DETR [2], utilize a full-size CNN backbone to provide low-level visual features required by the subsequent self-attention layers. Hierarchical architectures typically alternate self-attention and convolutional layers to form a mixed-hierarchical structure, aiming at fully utilizing the specialty of CNNs and Transformers, such as CvT [29], CMT [9], and MobileViT [18]. On the other hand, dual-branch architectures mainly focuses on reusing and fusing features from self-attention and convolutional branches [20]. Nevertheless, the aforementioned methods either disrupt the inductive bias of CNNs or introduce extra layers and parameters, posing additional challenges in model training. Conversely, this paper presents a novel horizontally scalable architecture that preserves the inductive bias in CNNs to the greatest extent and reduces training overheads.

Distributed Machine Learning: Distributed machine learning typically involves training large models on large-scale datasets and distributing the workload to numerous nodes [28]. Model parallelism and data parallelism are two primary strategies, which distribute the model architecture or the training data to several nodes to maximize computational efficiency and accelerate training [23, 28]. Besides, there are distributed machine learning approaches, like federated learning, that aim at preserving data privacy and are suitable for training models on sensitive or decentralized datasets [34]. In contrast to the aforementioned general-purpose distributed machine learning methods, this study specifically crafts a distributed

hybrid ViT architecture to accelerate training and inference processes on computing clusters.

3 PROPOSED MODEL

This section elucidates HsviT from three perspectives: feature processing pipeline, image-level feature embedding, and horizontally scalable self-attention.

3.1 Feature Processing Pipeline

The feature processing pipeline of HsviT is shown in Fig. 3. Initially, multiple convolutional kernels, each with a single output channel, are employed to extract features from the input image concurrently. The rationale behind this design is that each convolutional kernel captures one certain feature, and many of them construct the entire feature map needed for making a final prediction. Therefore, convolutional kernels are grouped and computed at different nodes to better utilize computational resources on clusters and extract the most possible number of features. Assuming there are K nodes in the cluster and each of them processes N features, the total number of features handled by the cluster is $K \times N$. Fig. 3 shows the case with $K = 3$. With the help of pooling layers, the feature map from each kernel is downsampled by Q and flattened as an image-level feature embedding. As shown in Fig. 3, after downsampling an image with size $3 \times H \times W$ by $Q = 2$, the size of image-level feature embeddings becomes $3N \times H/2 \times W/2$.

It is easy to divide image-level embeddings into non-overlapping attention groups, as each embedding contains the compressed spatial relationship of a certain feature in an image. As shown in Fig. 3, the feature embeddings are divided into 3 attention groups, with

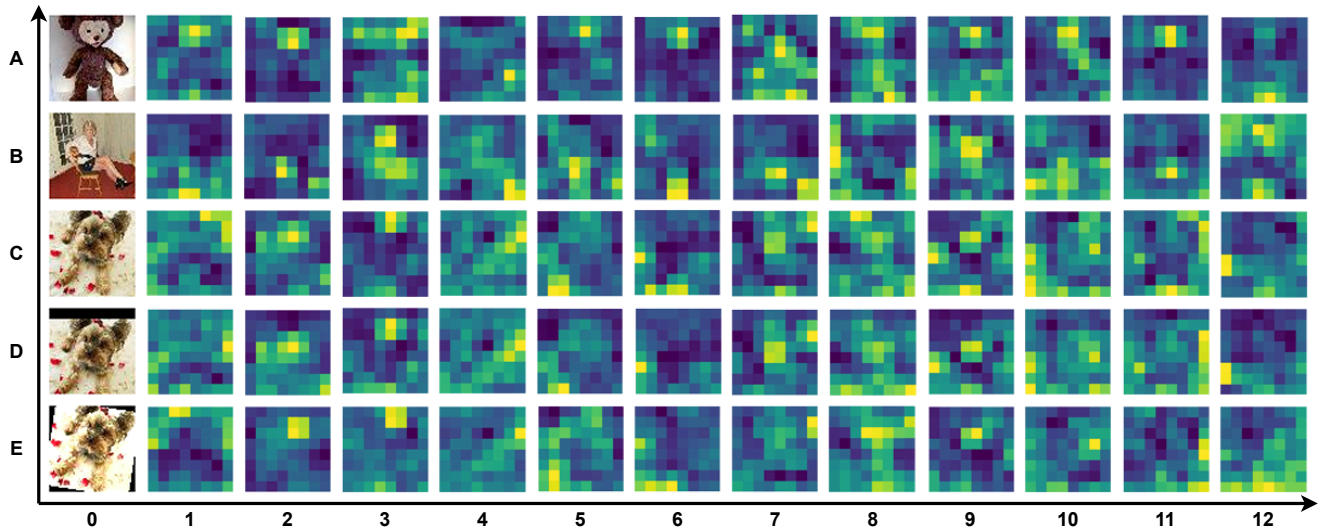


Figure 4: Visualized feature maps of the last convolutional layer in HSViT when testing on Tiny-ImageNet.

each of them having the shape of $N \times H/2 \times W/2$. Similar to the design in ViT [8], each attention group adds a CLS token for prediction. Therefore, each attention group possesses tokens with shape $(1+N) \times H/2 \times W/2$. After K nodes have calculated self-attentions in their respective attention groups, the generated CLS tokens are aggregated by average pooling, and fed into a Fully Connected (FC) layer for final prediction.

3.2 Image-Level Feature Embedding

To verify the idea of image-level feature embeddings, the feature maps after convolutional layers are visualized, as shown in Fig. 4. In particular, each row is an input image and its corresponding feature maps that are fed to the attention groups. In our experiments, the convolutional feature maps are divided into 16 attention groups. However, only the first 12 feature maps are presented in Fig. 4 due to the space limitation. It can be observed that convolutional layers enable the features in the original image to be downsampled from 64×64 to 8×8 , while maintaining the relative position of key features. As rows A, B, and C in Fig. 4 illustrate, different attention groups focus on different aspects of the same image. For example, feature maps A1 and A2 primarily focus on the face of the teddy bear, while feature maps A3, A7, and A8 mainly focus on the ears, arms, and legs. Besides, attentions are given to the salient object and the background, respectively, as indicated by B3 and B12. These demonstrate that HSViT effectively utilizes the convolutional features in a distributed manner, wherein more attention groups contribute to constructing attention on more distinct details and contexts.

Rows C, D, and E in Fig. 4 show that convolutional layers are shift-invariant and rotate-invariant, as the feature maps accurately reflect the relative positions of key features in augmented images. Without dividing the feature map into patches or encoding with extra position embeddings, image-level feature embeddings help each attention group comprehend a particular feature on their

feature maps. For example, in Fig. 4, C2, D2, and E2 illustrate that the convolutional layers accurately extract the facial features of the dog, help Attention Group 2 focus on encoding this dog-face feature and pay less attention to the context. By the same token, C9, D9, and E9 suggest a high probability of the dog-nose feature being activated and encoded by Attention Group 9.

3.3 Horizontally Scalable Self-Attention

As shown in Fig. 1, the horizontally scalable (d) design in HSViT is different from conventional convolutional backbone (a), hierarchical (b), and dual-branch (c) designs. In particular, the horizontally scalable design employs numerous small convolutional layers and self-attention layers to extract features simultaneously, enabling HSViT to make its final prediction with a voting-like mechanism. As shown in Fig. 3, after each attention group has generated its prediction embedding (CLS token), the prediction embeddings are aggregated using average pooling. Prediction embeddings from the majority of attention groups will significantly influence the final choice if they contain strong signals indicating the class to which the image belongs. As an example, on Row A of Fig. 4, the attention groups A1, A2, A5, A6, and A11 identify the face and ears of the teddy bear, whereas A3, A7, and A8 identify the fluffy material and body shapes of the teddy bear. These prediction embeddings with strong signals toward the teddy bear allow HSViT to reach a final prediction of the teddy bear class on the image.

Due to its distributed feature extraction design, HSViT lessens the necessity for extremely deep convolutional and self-attention layers, reducing the size of every convolution and self-attention module. Fig. 1 illustrates the distinction by plotting relatively smaller convolutional modules and self-attention modules than those from traditional architectures. Another advantage of the horizontally scalable design is high adaptability. At certain costs of performance, it is easy to reduce the model size by reducing the number of attention groups (and the corresponding convolutional kernels). The

high adaptability enables HSViT to adapt to edge devices with constrained computational resources, while allowing it to be trained on supercomputers and clusters.

4 EXPERIMENTS

This section presents the experiments with regard to implementation, image classification performance, ablation studies, sensitivity analysis, and further discussion.

4.1 Implementation

Table 1: Model Variants.

	Input Size		
	32 × 32	64 × 64	128 × 128
	Block Design, [Output/Embedding Size]		
C2A2	CB, [16 × 16]	CB, [16 × 16]	CB, [32 × 32]
	CB, [8 × 8]	CB, [8 × 8]	CB, [8 × 8]
	2 × MHSA, [64]	2 × MHSA, [64]	2 × MHSA, [64]
C3A4	CB, [16 × 16]	CB, [32 × 32]	CB, [32 × 32]
	CB, [16 × 16]	CB, [16 × 16]	CB, [16 × 16]
	CB, [8 × 8]	CB, [8 × 8]	CB, [8 × 8]
	4 × MHSA, [64]	4 × MHSA, [64]	4 × MHSA, [64]
C4A8	CB, [16 × 16]	CB, [32 × 32]	CB, [64 × 64]
	CB, [16 × 16]	CB, [16 × 16]	CB, [32 × 32]
	CB, [8 × 8]	CB, [8 × 8]	CB, [16 × 16]
	CB, [8 × 8]	CB, [8 × 8]	CB, [8 × 8]
	8 × MHSA, [64]	8 × MHSA, [64]	8 × MHSA, [64]

¹CB: Convolutional Block.

²MHSA: Multi-Head Self-Attention Block.

Model Variants: The proposed HSViT scheme involves multiple hyperparameters, such as the number of convolutional kernels, convolutional layers, attention groups, convolutional layer depth, and attention layer depth. To conduct a thorough comparison with the state-of-the-art schemes, three sizes of HSViT models are designed: HSViT-C2A2, HSViT-C3A4, and HSViT-C4A8, where the number in the name indicates the number of convolutional blocks and multi-head self-attention blocks of each model. Each convolutional block includes two Conv2d layers and one max-pooling layer. Each MHSA block includes one multi-head self-attention operation. As the convolutional layers get deeper, more convolutional kernels are required for extracting more distinct features. As a result, the number of kernels for convolutional blocks is set to 64, 128, 256, and so on if there are any. For all model variants, the embedding size is set to 64 (flattened by an 8 × 8 feature map) for the self-attention layers to obtain sufficient convolutional features and their relative location information. By default, the number of attention groups is set to 16. Table 1 depicts detailed building block designs of the variant models.

Datasets: To validate the effectiveness of HSViT in preserving inductive biases from convolutional layers, only small datasets are utilized to train the models from scratch. In particular, five image classification datasets, each containing fewer than 200,000 samples in total, are utilized to evaluate the performance of the proposed HSViT, including CIFAR-10 [12], CIFAR-100 [12], Fashion-MNIST [32], Tiny-ImageNet [30], and Food-101 [1]. For certain

models that do not support small input sizes, the image size is upsampled to ensure proper training. Table 2 illustrates the specifications of the datasets in detail.

Table 2: Dataset Specifications.

Dataset	# Classes	# Samples	Image Size
CIFAR-10	10	60,000	32 × 32
CIFAR-100	100	60,000	32 × 32
Fashion-MNIST	10	60,000	28 × 28
Tiny-ImageNet	200	120,000	64 × 64
Food-101	101	101,000	128 × 128

Training Details: The proposed models are implemented on the PyTorch [21] framework. AdamW [17] is adopted as the optimizer, with the learning rate set to 0.001 and the weight decay set to 0.01 by default. The learning rate is adjusted through the cosine annealing method. All models are trained from scratch for 300 epochs with a batch size of 512 on a Nvidia RTX 4090 GPU.

4.2 Image Classification

Table 3 compares the image classification performance of the proposed HSViT models with the state-of-the-art CNN, ViT, and Hybrid ViT models. In particular, for CNNs, the famous ResNet [10], EfficientNet [26], and MobileNetV2 [24] are used as benchmark models. The classic ViT [8] model is also incorporated as a patch-level feature embedding performance benchmark. However, this paper does not contain other ViT variations because they usually require pre-training to perform well on downstream tasks. As highly relative to the Hybrid ViT models, the recently introduced MobileViT [18], EfficientFormer [13], SwiftFormer [25], and CvT [29] are included for a thorough comparison.

Compared with the state-of-the-art schemes with similar parameter numbers, HSViT achieves higher top-1 accuracy due to its better preservation of inductive bias from convolutional layers. For example, on Tiny-ImageNet, HSViT-C3A4 achieves 56.73% top-1 accuracy with 2.3 M parameters, surpassing SwiftFormer-XS by 4.76% (3.1 M, 51.97%), MobileViT-XS by 2.84% (2.0 M, 53.89%), and MobileNetV2-1.0 by 8.66% (2.5 M, 48.07%). With 6.9 M parameters, HSViT-C4A8 achieves the highest top-1 accuracy among the five datasets, except for Fashion-MNIST, where it shares the same 95.92% accuracy as ResNet-50.

It is noteworthy that HSViT-C2A2 manages to decrease the number of model parameters to 0.8 M without utilizing depthwise separable convolution techniques in MobileNet. This reduction is primarily achieved by reducing the number of layers of the model. However, HSViT-C2A2 still achieves higher top-1 accuracy than CvT-13 and CvT-21 among the five datasets when training from scratch, indicating that HSViT better retains the inductive bias of convolutional layers, even when the number of layers is greatly decreased.

It can be observed that certain schemes show a decreased top-1 accuracy after increasing the model size. For instance, MobileViT-S (5.1 M, 68.00%) has a lower top-1 accuracy than MobileViT-XS (2.0 M, 75.45%) on Food-101. EfficientNet-B3 (11.0 M, 48.85%) is inferior

Table 3: Comparison of Top-1 Accuracy (%) with State-of-the-Art Schemes.

Model	# Layers ¹	# Param. ²	Top-1 Accuracy (%)					
			CIFAR-10	CIFAR-100	Fashion-MNIST	Tiny-ImageNet	Food-101	
CNN	ResNet-18	20 + 0	11.3 M	92.56	69.08	95.63	52.42	69.36
	ResNet-50	53 + 0	23.9 M	93.69	71.03	95.92	56.02	74.78
	EfficientNet-B0	81 + 0	4.3 M	90.69	68.41	95.26	50.17	73.55
	EfficientNet-B3	130 + 0	11.0 M	90.57	68.77	87.17	48.85	73.65
	MobileNetV2-1.0	37 + 0	2.5 M	92.12	66.25	95.22	48.07	69.58
	MobileNetV2-1.4	37 + 0	4.7 M	92.62	69.62	95.74	54.12	75.85
ViT	ViT-B ³	0 + 12	85.4 M	83.33	62.10	93.55	55.51	73.64
Hybrid	MobileViT-XS	35 + 9	2.0 M	93.09	70.83	95.53	53.89	75.45
	MobileViT-S	35 + 9	5.1 M	92.87	70.97	95.73	55.73	68.00
	EfficientFormer-L1	33 + 1	11.6 M	92.57	72.79	95.87	56.29	75.28
	EfficientFormer-L3	49 + 4	30.6 M	93.34	73.82	95.71	58.99	77.21
	SwiftFormer-XS	61 + 4	3.1 M	92.34	68.19	95.61	51.97	69.82
	SwiftFormer-S	76 + 4	5.7 M	92.56	68.23	95.87	52.81	71.12
	CvT-13	16 + 13	19.7 M	87.91	63.32	94.76	49.97	61.44 ³
	CvT-21	24 + 21	31.3 M	87.65	61.93	94.89	47.40 ³	62.21
Ours	HSViT-C2A2	4 + 2	0.8 M	90.64	67.84	95.10	50.50	67.88
	HSViT-C3A4	6 + 4	2.3 M	93.04	72.46	95.72	56.73	73.54
	HSViT-C4A8	8 + 8	6.9 M	94.04	73.85	95.92	59.25	79.06

¹The number of layers is recorded in the format of Conv2d + Attention.

²The number of parameters is calculated when training models on Tiny-ImageNet with image size 64×64 .

³The learning rate is adjusted to 1×10^{-4} for convergence.

to EfficientNet-B0 (4.3 M, 50.17%) on Tiny-ImageNet. This phenomenon occurs because the deeper layers or larger embeddings in the models present additional challenges to training, especially on small datasets. By contrast, the shallow layers in HSViT allow it to be trained more easily, while the proposed horizontal scalability allows the model to learn more features by employing more convolutional kernels.

4.3 Ablation Studies

Table 4: Ablation Study on CIFAR-10 and CIFAR-100.

Model	Module		Top-1 Accuracy (%)	
	Attn	Conv2d	CIFAR-10	CIFAR-100
HSViT-C2A2	✓		60.43	32.29
		✓	87.36	37.92
	✓	✓	90.64	67.84
HSViT-C3A4	✓		63.52	35.17
		✓	91.87	42.83
	✓	✓	93.04	72.46
HSViT-C4A8	✓		64.73	37.29
		✓	93.32	43.51
	✓	✓	94.04	73.85

¹Modules without the "✓" mark are ablated.

Ablate Self-Attention Module: On CIFAR-10 and CIFAR-100, the top-1 accuracy of HSViT declines with the ablation of the self-attention module. In particular, as shown in Table 4, on CIFAR-10, as the number of convolutional blocks grows (from C2 to C4), the

ablation of the self-attention module has a decreasing effect on the top-1 accuracy, from 3.28% to 0.72%. However, the phenomenon is not obvious on CIFAR-100. Although C2 and C4 have different numbers of convolutional blocks, the ablation of the self-attention module consistently results in a 30% reduction in top-1 accuracy. The reason is that C4 alone offers enough convolutional layers to extract and aggregate features from CIFAR-10, resulting in an acceptable top-1 accuracy of 93.32%. However, C4 alone has insufficient feature aggregation capability and understanding in handling CIFAR-100, as the number of classes is increased to ten times while the number of samples for each class is reduced to a tenth. Comparing the absolute drop in the top-1 accuracy between CIFAR-10 and CIFAR-100 after ablating the self-attention module further supports this insight. Take HSViT-C2A2 as an example, the reduction is 3.28% for CIFAR-10 but is 29.92% for CIFAR-100, indicating that the self-attention module imparts a richer comprehension of the CIFAR-100 features to HSViT.

Ablate Convolutional Module: Ablating the convolutional module from HSViT reveals a significant drop in top-1 accuracy of approximately 30% and 36% for CIFAR-10 and CIFAR-100, respectively. This drop demonstrates that the image-level convolutional kernel is necessary to extract useful features for the latter self-attention module. In addition, the convolutional module consistently has a more significant impact on the top-1 accuracy than the self-attention module. In particular, for HSViT-C4A8 on CIFAR-10, when ablating convolutional and self-attention modules, the top-1 accuracy reduction is 29.31% vs. 0.72%. This phenomenon is because insufficient data prevents the self-attention module from learning to pay attention to local features, which makes it highly dependent on convolutional layers for extracting local information, as pointed out

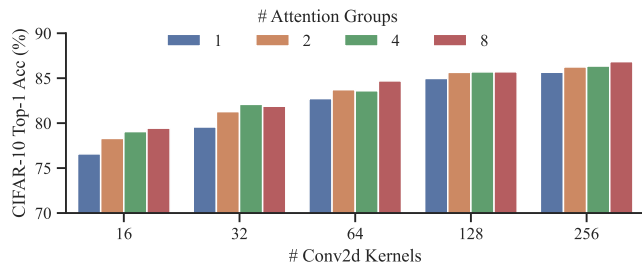


Figure 5: Number of convolutional kernels vs. number of attention groups. As the number of convolutional kernels and attention groups grows, the top-1 accuracy on CIFAR-10 rises.

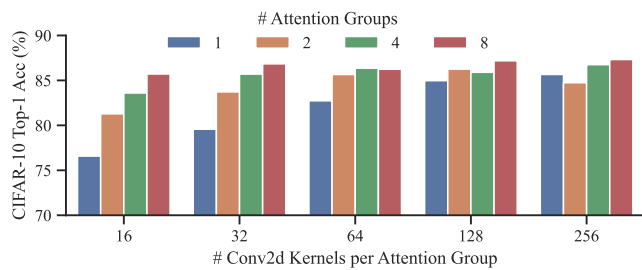


Figure 6: Number of convolutional kernels per attention group vs. number of attention groups. The top-1 accuracy on CIFAR-10 plateaus once the model has learned a sufficient number of features, irrespective of the increase of convolutional kernels or attention groups.

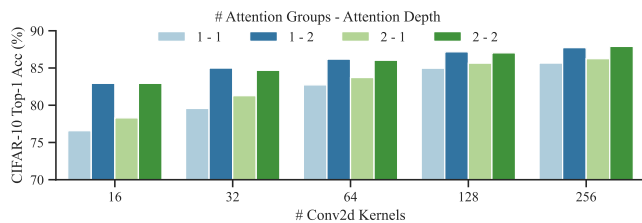


Figure 7: Number of attention groups and attention depth. A deeper self-attention module compensates for the reduced number of attention groups in feature understanding.

in [22]. Nevertheless, the effectiveness of the self-attention module is also considerable, as it offers a useful understanding of various features and improves top-1 accuracy with only a few layers of parameters, particularly when the classification task becomes more complicated, like CIFAR-100.

4.4 Sensitivity Analysis

Convolutional Kernels and Attention Groups: As shown in Fig. 5, the top-1 accuracy on CIFAR-10 increases as the number of convolutional kernels or attention groups increases. The phenomenon is consistent with intuition. Specifically, the more convolutional

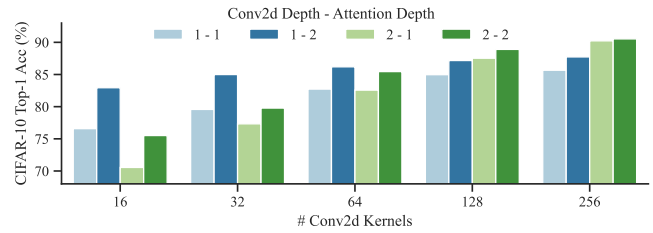


Figure 8: Convolution depth and attention depth. More convolutional kernels necessitate both deeper convolutional and deeper self-attention layers to achieve optimal accuracy.

kernels indicate more features extracted in the convolutional layers, facilitating the discrimination of local details on images. On the other hand, an increased number of attention groups implies a more delicate understanding of the extracted convolutional features and more stands in the voting stage, leading to a more accurate final prediction. Nonetheless, the increase in top-1 accuracy will level off once the number of convolutional kernels and attention groups reaches a certain threshold, as the model has learned adequate features given its depth. As an example, as shown in Fig. 6, top-1 accuracy rises as predicted when the number of convolutional kernels for each attention group is increased from 16 to 32, but the growth becomes insignificant after 64. Likewise, when increasing the attention groups, the rise in top-1 accuracy becomes erratic beyond 64 convolutional kernels per attention group and plateaus at around 87%.

Attention Depth and Convolution Depth: Fig. 7 illustrates that a deeper attention module always improves top-1 accuracy, despite the improvement becoming less apparent as the number of convolutional kernels increases. This is because network depth is of crucial importance in integrating and enriching different levels of features, as evidenced in [10]. Noticeably, Fig. 7 shows that the number of attention groups has minimal effect on top-1 accuracy once the self-attention layers are increased to two. For example, when there are 64 convolutional kernels and only one self-attention layer, the top-1 accuracy difference between one and two attention groups is obvious, at around 1%. But when introducing two self-attention layers, the difference decreases to 0.15%. This phenomenon reveals that deeper self-attention modules help to understand the image-level convolutional features and even compensate for the decrease in attention groups. Fig. 8 shows the different impacts of convolution depth and attention depth on top-1 accuracy. In particular, the deeper attention module always improves top-1 accuracy, while the deeper convolution module only yields a positive effect when there is a sufficient number of convolutional kernels. This phenomenon is because the first layer has half as many convolutional kernels as the second layer. When the number of convolutional kernels is relatively small, the inadequate feature representation capacity in the first layer hinders the second layer from delivering enough features for the final prediction. Fig. 8 reveals that deeper convolutional layers, deeper self-attention layers, and a sufficient number of convolutional kernels collaboratively improve the performance of HSViT.

4.5 Discussion

Large numbers of convolutional kernels are observed to cause high Floating Point Operations (FLOPs), even though HSViT effectively reduces model parameters. Nevertheless, using depthwise separable convolution as in MobileNet [24] to further lower the parameter and FLOPs is promising. Besides, due to the horizontally scalable design, the distributed deployment on multiple devices could further mitigate the challenge.

Another challenge is increasing the resolution of the image-level feature embedding and identifying small objects in large images. This inevitably results in an expanded feature map and causes a quadratic increase in computational complexity within the self-attention module. A feasible approach is crowdsourcing, where large images are segmented into smaller sections and distributed across various attention groups (nodes) when a sufficient number of computing nodes are available in the network.

5 CONCLUSION

This paper introduces a horizontally scalable vision transformer (HSViT) scheme with a novel image-level feature embedding. The design of HSViT preserves the inductive bias from convolutional layers while effectively reducing the number of layers and parameters of the models. Besides, HSViT offers a novel method for joint training and inference of ViT models on resource-constrained devices. A series of experiments demonstrate that, without pre-training on large-scale datasets, HSViT surpasses state-of-the-art schemes, affirming its superior retention of inductive bias. Future work encompasses expanding HSViT to large-scale datasets and other computer vision tasks.

REFERENCES

- [1] Lukas Bossard, Matthieu Guillaumin, and Luc Van Gool. 2014. Food-101 – Mining Discriminative Components with Random Forests. In *European Conference on Computer Vision*.
- [2] Nicolas Carion, Francisco Massa, Gabriel Synnaeve, Nicolas Usunier, Alexander Kirillov, and Sergej Zagoruyko. 2020. End-to-end object detection with transformers. In *European conference on computer vision*. Springer, 213–229.
- [3] Chi-Chih Chang, Yuan-Yao Sung, Shixing Yu, Ning-Chi Huang, Diana Marculescu, and Kai-Chiang Wu. 2024. FLORA: Fine-grained Low-Rank Architecture Search for Vision Transformer. In *Proceedings of the IEEE/CVF Winter Conference on Applications of Computer Vision*. 2482–2491.
- [4] Dimitris Chatzopoulos, Carlos Bermejo, Zhanpeng Huang, and Pan Hui. 2017. Mobile augmented reality survey: From where we are to where we go. *Ieee Access* 5 (2017), 6917–6950.
- [5] Tianlong Chen, Yu Cheng, Zhe Gan, Lu Yuan, Lei Zhang, and Zhangyang Wang. 2021. Chasing sparsity in vision transformers: An end-to-end exploration. *Advances in Neural Information Processing Systems* 34 (2021), 19974–19988.
- [6] Xiangning Chen, Cho-Jui Hsieh, and Boqing Gong. 2022. When Vision Transformers Outperform ResNets without Pre-training or Strong Data Augmentations. In *International Conference on Learning Representations*.
- [7] Yinpeng Chen, Xiyang Dai, Mengchen Liu, Dongdong Chen, Lu Yuan, and Zicheng Liu. 2020. Dynamic convolution: Attention over convolution kernels. In *Proceedings of the IEEE/CVF conference on computer vision and pattern recognition*. 11030–11039.
- [8] Alexey Dosovitskiy, Lucas Beyer, Alexander Kolesnikov, Dirk Weissenborn, Xiaohua Zhai, Thomas Unterthiner, Mostafa Dehghani, Matthias Minderer, Georg Heigold, Sylvain Gelly, et al. 2021. An Image is Worth 16x16 Words: Transformers for Image Recognition at Scale. In *International Conference on Learning Representations*.
- [9] Jianyuan Guo, Kai Han, Han Wu, Yehui Tang, Xinghao Chen, Yunhe Wang, and Chang Xu. 2022. Cmt: Convolutional neural networks meet vision transformers. In *Proceedings of the IEEE/CVF Conference on Computer Vision and Pattern Recognition*. 12175–12185.
- [10] Kaiming He, Xiangyu Zhang, Shaoqing Ren, and Jian Sun. 2016. Deep residual learning for image recognition. In *Proceedings of the IEEE conference on computer vision and pattern recognition*. 770–778.
- [11] Mohammad Ashrafuol Hoque, Matti Siekkinen, and Jukka K Nurminen. 2012. Energy efficient multimedia streaming to mobile devices—A survey. *IEEE Communications Surveys & Tutorials* 16, 1 (2012), 579–597.
- [12] Alex Krizhevsky. 2009. *Learning multiple layers of features from tiny images*. Technical Report.
- [13] Yanyu Li, Geng Yuan, Yang Wen, Ju Hu, Georgios Evangelidis, Sergey Tulyakov, Yanzhi Wang, and Jian Ren. 2022. Efficientformer: Vision transformers at mobilenet speed. *Advances in Neural Information Processing Systems* 35 (2022), 12934–12949.
- [14] Ze Liu, Han Hu, Yutong Lin, Zhuliang Yao, Zhenda Xie, Yixuan Wei, Jia Ning, Yue Cao, Zheng Zhang, Li Dong, et al. 2022. Swin transformer v2: Scaling up capacity and resolution. In *Proceedings of the IEEE/CVF conference on computer vision and pattern recognition*. 12009–12019.
- [15] Ze Liu, Yutong Lin, Yue Cao, Han Hu, Yixuan Wei, Zheng Zhang, Stephen Lin, and Baining Guo. 2021. Swin transformer: Hierarchical vision transformer using shifted windows. In *Proceedings of the IEEE/CVF international conference on computer vision*. 10012–10022.
- [16] Zhenhua Liu, Yunhe Wang, Kai Han, Wei Zhang, Siwei Ma, and Wen Gao. 2021. Post-training quantization for vision transformer. *Advances in Neural Information Processing Systems* 34 (2021), 28092–28103.
- [17] Ilya Loshchilov and Frank Hutter. 2019. Decoupled Weight Decay Regularization. In *International Conference on Learning Representations*.
- [18] Sachin Mehta and Mohammad Rastegari. 2022. MobileViT: Light-weight, General-purpose, and Mobile-friendly Vision Transformer. In *International Conference on Learning Representations*.
- [19] Kaoru Ota, Minh Son Dao, Vasileios Mezaris, and Francesco GB De Natale. 2017. Deep learning for mobile multimedia: A survey. *ACM Transactions on Multimedia Computing, Communications, and Applications (TOMM)* 13, 3s (2017), 1–22.
- [20] Xuran Pan, Chunjiang Ge, Rui Lu, Shiji Song, Guanfu Chen, Zeyi Huang, and Gao Huang. 2022. On the integration of self-attention and convolution. In *Proceedings of the IEEE/CVF conference on computer vision and pattern recognition*. 815–825.
- [21] Adam Paszke, Sam Gross, Francisco Massa, Adam Lerer, James Bradbury, Gregory Chanan, Trevor Killeen, Zeming Lin, Natalia Gimelshein, Luca Antiga, et al. 2019. Pytorch: An imperative style, high-performance deep learning library. *Advances in neural information processing systems* 32 (2019).
- [22] Maithra Raghu, Thomas Unterthiner, Simon Kornblith, Chiyuan Zhang, and Alexey Dosovitskiy. 2021. Do vision transformers see like convolutional neural networks? *Advances in Neural Information Processing Systems* 34 (2021), 12116–12128.
- [23] Jeff Rasley, Samyam Rajbhandari, Olatunji Ruwase, and Yuxiong He. 2020. Deep-speed: System optimizations enable training deep learning models with over 100 billion parameters. In *Proceedings of the 26th ACM SIGKDD International Conference on Knowledge Discovery & Data Mining*. 3505–3506.
- [24] Mark Sandler, Andrew Howard, Menglong Zhu, Andrey Zhmoginov, and Liang-Chieh Chen. 2018. Mobilenetv2: Inverted residuals and linear bottlenecks. In *Proceedings of the IEEE conference on computer vision and pattern recognition*. 4510–4520.
- [25] Abdelrahman Shaker, Muhammad Maaz, Hanoona Rasheed, Salman Khan, Ming-Hsuan Yang, and Fahad Shahbaz Khan. 2023. SwiftFormer: Efficient Additive Attention for Transformer-based Real-time Mobile Vision Applications. In *Proceedings of the IEEE/CVF International Conference on Computer Vision (ICCV)*. 17425–17436.
- [26] Mingxing Tan and Quoc Le. 2019. Efficientnet: Rethinking model scaling for convolutional neural networks. In *International conference on machine learning*. PMLR, 6105–6114.
- [27] Ashish Vaswani, Noam Shazeer, Niki Parmar, Jakob Uszkoreit, Llion Jones, Aidan N Gomez, Łukasz Kaiser, and Illia Polosukhin. 2017. Attention is all you need. *Advances in neural information processing systems* 30 (2017).
- [28] Joost Verbraeken, Matthijs Wolting, Jonathan Katzky, Jeroen Kloppenburg, Tim Verbelen, and Jan S Rellermeyer. 2020. A survey on distributed machine learning. *Acm computing surveys (csur)* 53, 2 (2020), 1–33.
- [29] Haiping Wu, Bin Xiao, Noel Codella, Mengchen Liu, Xiyang Dai, Lu Yuan, and Lei Zhang. 2021. Cvt: Introducing convolutions to vision transformers. In *Proceedings of the IEEE/CVF international conference on computer vision*. 22–31.
- [30] Jiayu Wu, Qixiang Zhang, and Guoxi Xu. 2017. *Tiny imagenet challenge*. Technical Report.
- [31] Zhuofan Xia, Xuran Pan, Shiji Song, Li Erran Li, and Gao Huang. 2022. Vision transformer with deformable attention. In *Proceedings of the IEEE/CVF conference on computer vision and pattern recognition*. 4794–4803.
- [32] Han Xiao, Kashif Rasul, and Roland Vollgraf. 2017. *Fashion-MNIST: a Novel Image Dataset for Benchmarking Machine Learning Algorithms*. arXiv:cs.LG/1708.07747 [cs.LG]
- [33] Chenhao Xu, Chang-Tsun Li, Yongjian Hu, Chee Peng Lim, and Douglas Creighton. 2023. Deep Learning Techniques for Video Instance Segmentation: A Survey. *arXiv preprint arXiv:2310.12393* (2023).
- [34] Chenhao Xu, Youyang Qu, Yong Xiang, and Longxiang Gao. 2023. Asynchronous federated learning on heterogeneous devices: A survey. *Computer Science Review*

- 50 (2023), 100595.
- [35] Fang Yu, Kun Huang, Meng Wang, Yuan Cheng, Wei Chu, and Li Cui. 2022. Width & depth pruning for vision transformers. In *Proceedings of the AAAI Conference on Artificial Intelligence*, Vol. 36. 3143–3151.
- [36] Haofei Zhang, Jiarui Duan, Mengqi Xue, Jie Song, Li Sun, and Mingli Song. 2022. Bootstrapping ViTs: Towards liberating vision transformers from pre-training. In *Proceedings of the IEEE/CVF Conference on Computer Vision and Pattern Recognition*. 8944–8953.